SATURN'S MICROWAVE SPECTRUM: IMPLICATIONS FOR THE ATMOSPHERE AND THE RINGS

M. J. Klein, M. A. Janssen, S. Gulkis and E. T. Olsen

Earth and Space Sciences Division, Jet Propulsion Laboratory
California Institute of Technology
Pasadena, California 91103

ABSTRACT

Measurements of Saturn's disk temperature are compiled to determine the planet's microwave spectrum from 1 mm to 100 cm wavelength. The data were adjusted to conform with a common flux density scale. A model of Saturn's rings is used to remove the effects of the rings from the atmospheric component at centimeter and decimeter wavelengths. Theoretical spectra for a number of convective atmospheric models were computed and compared with the observed spectrum. Radiative-convective models with approximately solar composition and with an effective temperature of ~89 K are in good agreement with the observations. The agreement between the observed and theoretical spectra is a strong indication that gaseous ammonia is present in Saturn's atmosphere. A good fit to the data is obtained with an ammonia mixing ratio of $\sim 5 \times 10^{-4}$. Lower values of the NH_3 mixing ratio can also provide a good fit provided an additional source of microwave opacity is present in Saturn's atmosphere. Liquid water droplets in the troposphere could provide a substantial microwave opacity. A comparison of the millimeter wavelength data with the "best-fitting" atmospheric spectrum indicates that the thermal component of the ring brightness temperature near 1 mm wavelength is ~25 K.

INTRODUCTION

Theoretical studies have shown that Saturn's microwave spectrum can be explained by thermal emission from the tropospheric region of an atmosphere with generally solar composition and with ammonia as the primary source of microwave

opacity (Gulkis *et al.*, 1969; Wrixon and Welch, 1970; Gulkis and Poynter, 1972; Ohring and Lacser, 1975). In all of these studies, the influence of the rings on the observed brightness temperatures was assumed to be negligible. Because the available data consisted almost entirely of observations made with very low spatial resolution, the microwave properties of the rings were virtually unknown. In recent years, measurements of the planet and rings have been made with radio interferometers operating at wavelengths from 0.8 to 21 cm. These new data provide strong constraints on the microwave properties of the rings and hence their influence on the microwave spectrum can now be estimated. In addition, the microwave flux-density scale, which is used to calibrate the planetary measurements, has been defined with better accuracy and over a larger wavelength interval than it was only a few years ago. In this paper we make use of the new data to re-analyze Saturn's microwave spectrum.

We have compiled a new list of the published measurements of Saturn's microwave disk temperature for wavelengths between 1 mm and 100 cm. The data are normalized to a uniform calibration scale and the effects (e.g., obscuration, scattering and emission) of the rings are computed for a simple model of the rings. Computed spectra for several atmospheric models are compared with the spectrum from 0.8 cm to 100 cm. The influence of the rings in this spectral region is found to be small and it can be removed with confidence. Two "best fit" models are determined, one with an NH_3 mixing ratio which is somewhat greater than a solar value, and the other with a solar-like NH_3 mixing ratio but with an additional opacity source near the 270 K level in the troposphere. When either of these atmospheric models are extended to millimeter wavelengths, the computed temperatures fall systematically below the observed disk temperatures. This result is explained if the thermal component of the ring brightness temperature, assuming both the A and B rings are uniformly bright, is ~25 K for wavelengths near 1 mm. Finally, we computed the vertical transmission loss that a probe communication link is likely to encounter as it penetrates Saturn's atmosphere.

SATURN'S MICROWAVE SPECTRUM

Data Normalization Factors

Our list of measurements of Saturn from 1 mm to 100 cm is given in Table 1. Because most of the observations were obtained with single antennas having low spatial resolution, the majority of the reported temperatures include the integrated flux density

Table 1. Saturn's Microwave Spectrum

(1)	(2)	(3)	(4)	(5)[a]	(6)[b]	(7)[c]	(8)[c]	Reference
λ	T_D	Error (rel, abs)	|B|	f_{CAL}	$f_\Omega(B)$	T_s/T_D^*	T_s	
(cm)	(K)	(K)	(deg)				(K)	
0.1	145	(7 , 14)	22.0	1.0	0.983	0.937	133.4	Werner *et al.* (1978)
0.12	140	(15 , 22)	10.2	0.940	0.996	1.007	132.0	Low and Davidson (1965)
0.14	194	(8 , 21)	26.6	0.983	0.975	0.888	165.2	Rather *et al.* (1974)
0.14	120	(- , 30)	20.0	1.070	0.985	0.911	115.3	Kostenko *et al.* (1971)
0.14	184	(6 , 13)	26.6	1.0	0.975	0.898	161.1	Courtin *et al.* (1977)
0.14	188	(5 , 14)	25.4	1.0	0.977	0.914	168.0	Courtin *et al.* (1977)
0.213	164	(5 , 12)	26.4	0.980	0.976	0.876	137.4	Ulich (1974)
0.309	148	(5 , 11)	21.0	1.0	0.984	0.973	141.7	Ulich *et al.* (1973)
0.33	150	(6 , -)	8.0	1.0	0.998	1.024	153.2	Epstein *et al.* (1970)
0.33	155	(3 , -)	16.2	1.0	0.990	1.016	156.0	Epstein (1978)
0.341	144	(2 , -)	10.5	1.0	0.996	1.043	149.5	Ulich (1978)
0.35	132	(6 , 13)	16.3	1.220	0.990	1.035	165.1	Pauliny-Toth and Kellermann (1970)
0.353	151	(3 , -)	25.2	1.0	0.978	0.939	138.6	Ulich (1978)
0.387	115	(3 , 15)	26.4	1.286	0.976	0.923	133.2	Voronov *et al.* (1974)
0.428	148	(7 , -)	25.9	1.0	0.977	0.932	134.7	Ulich (1978)
0.6	156	(7 , -)	25.9	1.0	0.977	0.955	145.4	Ulich (1978)
0.696	158	(4 , -)	10.1	1.0	0.996	1.053	165.7	Ulich (1978)
0.82	132	(4 , 9)	17.6	1.0	0.989	1.059	138.2	Kuzmin and Losovsky (1971)
0.833	147	(4 , 9)	24.9	1.0	0.978	*	144.0	Janssen and Olsen (1978)

Table 1. Saturn's Microwave Spectrum (contd.)

(1)	(2)	(3)	(4)	(5)[a]	(6)[b]	(7)[c]	(8)[c]	
λ	T_D	Error (rel, abs)	|B|	f_{CAL}	$f_\Omega(B)$	T_s/T_D^*	T_s	Reference
(cm)	(K)	(K)	(deg)				(K)	
0.845	151	(3 , 7)	17.7	0.980	0.988	1.056	154.5	Wrixon and Welch (1970)
0.95	127	(3 , 13)	4.0	1.087	0.999	1.028	141.8	Pauliny-Toth and Kellermann (1970)
0.955	135	(7 , -)	25.9	1.0	0.977	0.981	129.3	Ulich (1978)
0.955	136	(4 , 6)	22.0	1.0	0.983	1.037	138.6	Dent (1972)
0.955	126	(- , 6)	6.0	1.059	0.999	1.043	139.0	Hobbs and Knapp (1971)
1.176	131	(3 , 6)	17.7	0.980	0.988	1.073	136.1	Wrixon and Welch (1970)
1.265	127	(4 , 6)	18.4	0.980	0.988	1.074	132.0	Wrixon and Welch (1970)
1.304	139	(2 , 8)	23.6	0.918	0.981	*	125.0	Schloerb (1977)
1.463	131	(3 , 5)	17.0	1.0	0.989	1.084	140.4	Wrixon and Welch (1970)
1.53	141	(10 , 15)	10.2	0.967	0.996	1.070	145.4	Welch *et al.* (1966)
1.95	145	(4 , -)	4.0	0.938	0.999	1.038	141.1	Pauliny-Toth and Kellermann (1970)
2.07	162	(4 , 7)	26.5	1.0	0.976	1.020	161.2	Gary (1974)
3.12	137	(7 , 12)	6.2	1.053	0.999	1.043	150.3	Berge (1968)
3.56	170	(2 , 6)	26.5	1.0	0.976	1.011	167.7	Gary (1974)
3.56	158	(2 , 6)	17.9	1.0	0.988	1.091	170.3	Turegano and Klein (1978)
3.71	161	(5 , 7)	26.1	1.035	0.976	*	163.0	Cuzzi and Dent (1975)
3.71	171	(5 , -)	15.3	1.0	0.991	*	169.0	Schloerb (1977)
3.75	168	(7 , 11)	5.8	1.048	0.999	1.045	183.7	Seling (1970)
6.0	175	(17 , 19)	10.0	1.040	0.996	1.072	198.8	Kellermann (1966)

Table 1. Saturn's Microwave Spectrum (contd.)

(1)	(2)	(3)	(4)	(5)[a]	(6)[b]	(7)[c]	(8)[c]	
λ (cm)	T_D (K)	Error (rel, abs) (K)	$\|B\|$ (deg)	f_{CAL}	$f_\Omega(B)$	T_s/T_D^*	T_s (K)	Reference
6.0	190	(- , 45)	0.2	1.0	1.000	1.000	190.0	Hughes (1966)
6.2	162	(12 , 18)	24.8	1.037	0.978	1.044	171.6	Gerard and Kazes (1973)
9.0	165	(- , 25)	1.1	1.060	1.000	*	175.0	Berge and Read (1968)
10.0	196	(- , 44)	17.9	0.988	0.988	1.086	207.7	Drake (1962)
10.7	172	(- , 20)	5.4	1.061	0.999	*	182.0	Berge and Read (1968)
11.1	186	(20 , 25)	25.[illegible]	1.050	0.978	1.033	197.2	Gerard and Kazes (1973)
11.3	182	(4 , 18)	14.7	1.024	0.992	1.085	200.5	Davies *et al.* (1964)
11.3	196	(17 , 20)	8.0	1.025	0.998	1.056	211.6	Kellermann (1966)
21.1	208	(13 , -)	16.8	1.010	0.989	*	208.0	Berge and Muhleman (1973)
21.1	231	(9 , -)	21.8	0.978	0.983	*	222.0	Berge and Muhleman (1973)
21.1	230	(10 , 15)	25.2	0.988	0.978	*	222.0	Briggs (1973)
21.2	286	(10 , 37)	18.0	0.950	0.988	1.089	292.0	Davies and Williams (1966)
21.2	193	(20 , 25)	21.5	0.988	0.983	1.071	200.8	Gerard and Kazes (1973)
21.2	207	(20 , 25)	25.0	0.988	0.978	1.031	206.2	Gerard and Kazes (1973)
21.4	214	(14 , 15)	26.2	1.029	0.976	1.015	218.1	Condon *et al.* (1974)

Table 1. Saturn's Microwave Spectrum (contd.)

(1)	(2)	(3)	(4)	(5)[a]	(6)[b]	(7)[c]	(8)[c]	
λ	T_D	Error (rel, abs)	|B|	f_{CAL}	$f_\Omega(B)$	T_s/T_D^*	T_s	Reference
(cm)	(K)	(K)	(deg)				(K)	
49.5	390	(- , 65)	21.8	1.050	0.983	1.074	432.2	Yerbury *et al.* (1971)
69.7	385	(45 , 49)	26.3	1.0	0.976	1.019	382.8	Condon *et al.* (1974)
94.3	540	(- ,110)	24.7	1.0	0.979	1.040	549.6	Yerbury *et al.* (1973)

[a]The factor f_{CAL} is the multiplier used to normalize the observed disk temperatures to the microwave flux density scale of Baars, Genzel, Pauliny-Toth and Witzel (1977) for $100 > \lambda > 1$ cm; and the spectrum of DR-21 for $1 > \lambda > 0.3$ cm (Dent, 1972 ; B. L. Ulich private communication). For $\lambda < 0.3$ cm, we rely on the calibration of the most recent observations, and we normalize the older data to this calibration via the observed ratios of Saturn to Jupiter and Venus.

[b]The disk temperatures listed in column 2 are based on the solid angle given by the polar and equatorial semi-diameters of Saturn published in the AENA. The factor $f_\Omega(B)$ corrects this reference solid angle to the value for an oblate spheriod inclined to the observer at the angle B.

[c]The ratio T_s/T_D^* , where $T_D^* = T_D f_{CAL} f(B)$, is computed based on the ring model described in the text.

T_D^* is thus the equivalent disk temperature of the Saturn-ring system, adjusted to a common flux density scale and corrected for viewing geometry, while T_s is the average brightness temperature of the disk alone.

from both the planet and the rings. The temperatures given in the second column of the table are based on the assumption that all of the observed flux density is emitted from the solid angle of the apparent disk of Saturn, i.e., emission, scattering and obscuration by the rings was ignored for all but the nine interferometric observations. We treat the interferometric data separately because the influence of the rings was already removed by the authors. In the following discussion we describe the various correction factors we have applied to the original data to derive the final disk temperatures (Column 8), which represents the microwave spectrum of Saturn's atmosphere.

All of the observed temperatures were adjusted to a common flux-density scale given by Baars *et al.* (1977), and to the solid angle computed from the polar and equatorial semi-diameters given in the American Ephemeris and Nautical Almanac. The flux scale normalization factors, f_{CAL}, are listed in Column 5 of Table 1. An additional correction was applied to the data to account for the fact that the solid angle of an oblate spheriod varies with B, which is the angle the planet is tipped toward (or away from) the Earth at the time of the observation. The corresponding correction factors for the solid angle, $f_{\Omega}(B)$, are given in Column 6.

Influence of the Rings

To remove the influence of the rings from Saturn's microwave spectrum, we adopt a model for the microwave properties of the rings and use this model to derive correction factors to be applied to the single antenna measurements. These correction factors, given in Column 7, convert the measured disk temperatures, which include the influence of the rings, to the temperatures that would have been observed if there were no rings. We account for the finite beamwidth of the antenna used for each measurement. The latter correction is primarily important at the short wavelengths where the spatial resolution of antennas can be comparable to the angular size of Saturn's Ring system. The correction factors account for the weak thermal emission from the rings, for the fraction of thermal emission from Saturn's disk reflected off the rings, and for the attenuation of atmospheric emission transmitted through the sector of the rings which obscures the planet. The three components are schematically identified in Figure 1.

The nominal ring model incorporates the following assumptions and approximations. First, we assume that only the A and B rings are important to this discussion and that the microwave properties of these two rings are identical. We adopt $\tau = 0.7$

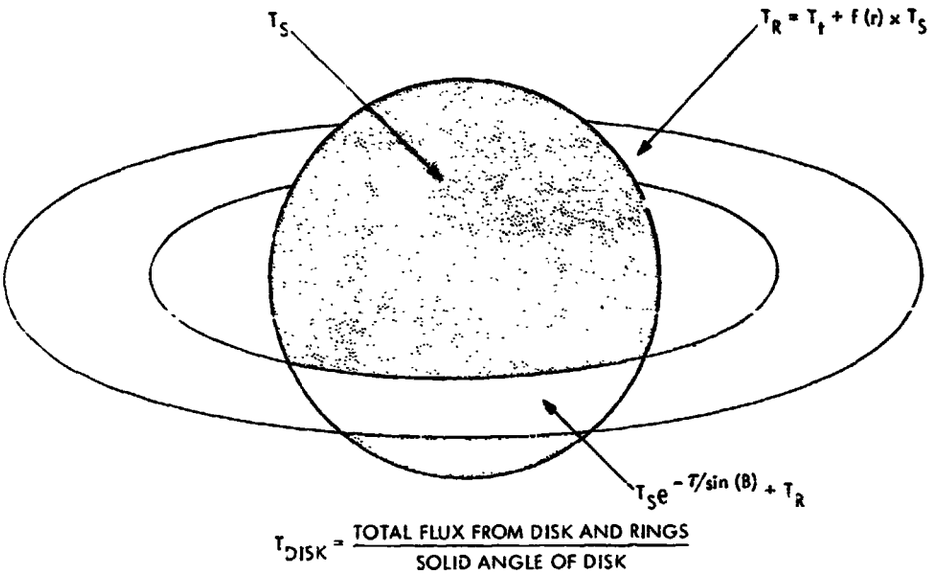

Figure 1. Schematic model of the brightness distribution of Saturn and the rings. Given the ring parameters T_r and τ, the brightness temperature, T_s, of Saturn's disk can be determined for any ring-inclination B. T_s is the temperature that would be measured in the absence of the rings.

for the optical depth of the rings at normal incidence and compute the absorption of the atmospheric emission by the obscuring sector of the rings (see Figure 1). We further assume that the opacity is independent of frequency over the microwave spectrum. These assumptions are based on the results of recent interferometric observations (Briggs, 1973; Berge and Muhleman, 1973; Cuzzi and Dent, 1975; Schloerb, 1977; Janssen and Olsen, 1978).

The ring brightness temperature, T_R is given by the sum of T_t and $f(r)T_S$, where T_t is the thermal brightness temperature of the rings, f(r) is an expression for the radial dependence of the reflected atmospheric temperature, T_S. The function f(r) is computed with the assumption that the rings form a perfectly-reflecting Lambertian-scattering surface. This assumption is an acceptable approximation to the more physically realistic models with multiple scattering computations (see e.g., Schloerb, 1977). The observational results for $\lambda > 1$ cm show that T_R is consistent with the reflected component as the primary source of brightness with the possibility of a small thermal component. For our nominal model, we set $T_t = 2 \pm 2$ K and calculate an average total ring contribution of $T_R \sim 7$ K. This choice encompasses the results of all interferometric measurements at centimeter wavelengths.

There is evidence that T_t increases with decreasing wavelength shortward of ~1 cm, but the wavelength dependence is strictly unknown. The computations of the

correction factors listed in the table are based on the assumption that T_t increases monotonically from $T_t \sim 7$ K near 8 mm (Janssen and Olsen, 1978) to $T_t \sim 25$ K near 1 mm wavelength. We show in a following section that this increase in T_t is consistent with the millimeter observations.

A computer program was written to calculate the disk temperature of the model illustrated in Figure 1 and described above. The brightness temperature T_S was adjusted to give the corrected disk temperature $T_D^* = T_D f_{CAL} f_\Omega(B)$. The corresponding correction factor T_S/T_D^* was then calculated for each single antenna observation in Table 1 and is listed in Column 7. The brightness temperature T_S (Column 8) is the disk temperature of Saturn which would be measured in the absence of rings.

ATMOSPHERIC MODELS

We computed theoretical microwave spectra for several models of Saturn's atmosphere to compare with the observational data. Each model is in hydrostatic equilibrium throughout, with the lower troposphere in convective equilibrium. The temperature-pressure profile in the upper stratosphere is given by the solution of the Eddington equation for a constant-flux, gray radiative atmosphere. The range of models is constrained by the effective temperature, T_e, that we allow in the solution. Current estimates of Saturn's effective temperature, derived from infrared observations, are near 90 K (e.g., Ward, 1977). We will restrict our discussion to three models which we designate Nominal (T_e = 89 K), Cool (T_e = 84 K) and Warm (T_e = 94 K).

The composition for each model is assumed to be primarily H_2 and He with CH_4, NH_3 and H_2O as minor constituents. The H_2, He and CH_4 are assumed uniformly mixed throughout the atmosphere with a He/H_2 number mixing ratio of 0.2 and $CH_4/H_2 = 2.1 \times 10^{-3}$ (Caldwell, 1977). Ammonia is assumed to be uniformly mixed in the troposphere and saturated in the upper troposphere. The partial pressure of saturated ammonia is controlled by the temperature according to the condensation relation

$$\text{Log } P_{NH_3} = 9.9974 - 1630\ T^{-1} \qquad (1)$$

where the pressure is in millimeters of Hg and T is degrees Kelvin.

The procedure for calculating the models begins with an initial estimate of a pressure-temperature point on an adiabat deep in the atmosphere (p > 10 atm). Solutions to the equation of hydrostatic equilibrium give the pressure at successively higher altitudes as the temperature decreases with the adiabatic gradient. For our choices of composition and gravitational acceleration (g = 905 cm^2 s^{-1}) the adiabatic gradient is ~0.97 K km^{-1}. Both the adiabatic lapse rate and a radiative lapse rate are calculated at each pressure point, until the adiabatic gradient overtakes the radiative gradient. Above this point, the temperature follows the radiative profile with increasing altitude. With this procedure, each pressure-temperature profile is uniquely specified either by a single pressure-temperature point or by the effective temperature. A more complete discussion of this procedure is given by Klein and Gulkis (1978).

The pressure-temperature profiles for our Warm, Nominal and Cool models are shown in Figure 2. The condensation temperatures for water and ammonia are marked to indicate the respective pressures where cloud bases are expected. The solid curves represent the convective portion of the atmosphere and the broken curves show the radiative regime. The thermal profile in and above the stratosphere does not

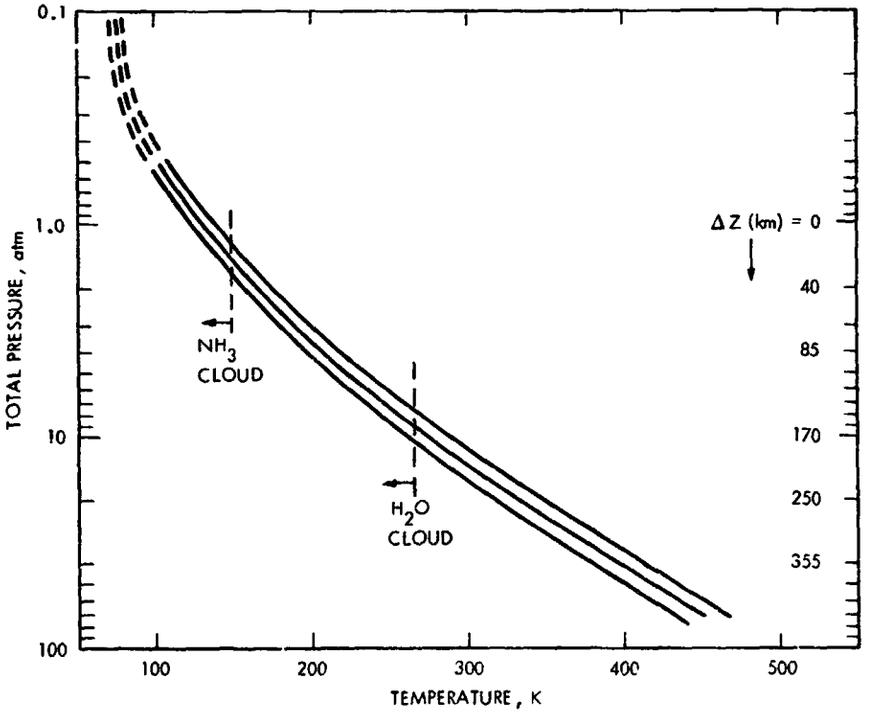

Figure 2. Pressure-Temperature profiles are shown for three atmospheric models of Saturn described in the text. The Cool, Nominal and Warm models correspond to the effective temperatures, respectively shown from left to right, T_e = 84K, 89K, 94K.

affect our interpretation of Saturn's microwave spectrum because the microwave opacity is very small in this region. For this reason we are not concerned with a temperature inversion which might form at high altitudes.

The atmospheric parameters, i.e., pressure, temperature and composition are related to the observed microwave brightness temperature through the equation of radiative transfer. The final step of our modeling program (see Klein and Gulkis, 1978) is to compute the distribution of the microwave brightness over the planet and from this we compute the mean brightness temperature of Saturn's oblate disk as a function of frequency. The resultant microwave spectrum for each model can then be compared with the spectrum, of the "ring free" temperature, T_S.

INTERPRETING THE SPECTRUM

The NH_3 Abundance

Among the various molecular species that have been detected or that are likely to be found in Saturn's atmosphere, ammonia is by far the most effective source of microwave opacity. For this reason, the observed microwave spectrum contains information on the average concentration and vertical distribution of ammonia on a global scale. In particular, the shape of the computed spectra corresponding to different atmospheric models depends upon our choice of $[NH_3]$, which is the number mixing ratio of ammonia at depth, and upon the pressure-temperature profile of each model. In this section the observed spectrum of Saturn's atmosphere is compared with the computed spectra for our Nominal model (T_e = 89 K). Several values of $[NH_3]$ are obtained and the sensitivity of the result to variations in other model assumptions is discussed.

For our study of the ammonia mixing ratio we concentrate on the spectral region from 0.8 to ~50 cm. Our confidence in both the ring-model corrections and the accuracy of the flux density scale is considerably greater for $\lambda > 8$ mm. The long-wavelength limit is imposed by the uncertainty of extrapolating microwave absorption coefficients to the deep atmosphere where pressures exceed 1000 atmospheres; emission from these regions begins to contribute significantly to the brightness temperature for wavelengths beyond ~50 cm. Exclusion of data at wavelengths longer than 50 cm minimizes the possible effects of non-thermal (synchrotron) emission from trapped radiation

belts. Condon *et al.* (1974) show that postulated components of synchrotron emission are insignificant for $\lambda \leq 21$ cm.

The measurements of Saturn's microwave spectrum for wavelengths >8 mm are plotted in Figure 3. Theoretical spectra for our Nominal model with selected values of $[NH_3]$ are represented by the four curves. It is evident that mixing ratios between 3×10^{-4} and 10×10^{-4} yield acceptable fits to the data. A formal analysis with weighted Chi-square tests gave an optimum abundance of $[NH_3] \sim 5 \times 10^{-4}$. For this analysis we included all data in the range $0.8 \leq \lambda \leq 21$ cm, each weighted by the square of the reciprocal of the relative error.

A constant multiplier, which was an additional free parameter in the analysis, allows for a uniform uncertainty in the absolute flux density scale. The minimum Chi-square solution was found with this constant equal to 0.96, which is consistent with this uncertainty. However, factors less than unity can also be explained (1) if we have underestimated the thermal emission from the rings; (2) if the ring opacity is less than 0.7; or (3) by atmospheric model assumptions that are invalid. One plausible example of the latter is the increase in disk temperature that occurs if the NH_3 is not completely saturated in the cloud regions. For example, the relative NH_3 humidity might differ from one area to the next on the disk (e.g., belts and zones).

The relative insensitivity of the computed spectra to nominal changes in T_e and the He abundance is demonstrated in Figures 4 and 5. The small changes in slope of the computed spectra that occur at the longer wavelengths can be compensated in the model by incrementing the value of $[NH_3]$ an insignificant amount.

Model with H_2O Cloud

Noting that atmospheric models predict the formation of a water cloud near the 270 K temperature region, one might ask if there is any evidence of such a cloud in Saturn's microwave spectrum. To investigate this possibility, we added a variable opacity term to our model near the 270 K level and recalculated the microwave spectrum for the Nominal pressure-temperature model. The ammonia mixing ratio was reduced to 1.5×10^{-4} to bring it into agreement with the solar N abundance. The microwave opacity in the "cloud" region was assumed to be $\tau_{cl} = \tau_o \nu^{-2}$, where $\tau_o = 1$ at 1 GHz and ν is the frequency in GHz. Our choice of opacity is based on the microwave absorption of small (<1 mm) water droplets and a cloud density of ~ 35 g m^{-3}

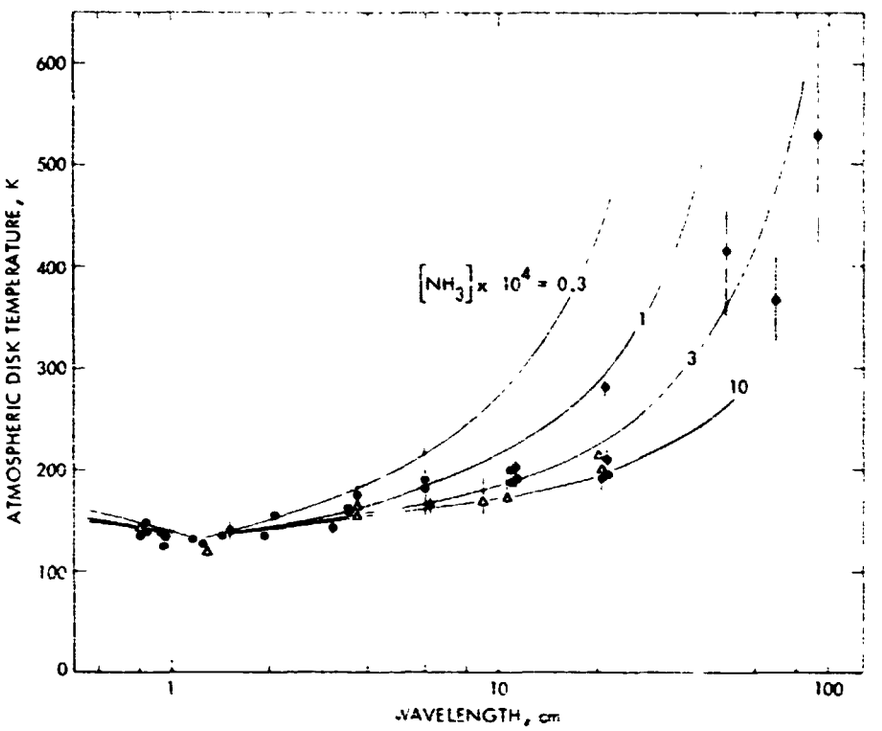

Figure 3. The microwave spectrum of Saturn's atmospheric temperature in the wavelength interval 0.8 to 100 cm. The filled circles represent single antenna data which have been adjusted slightly to remove the influence of the rings. The eight triangles represent the interferometric measurements which do not require ring corrections. The four curves represent the computed spectra for our Nominal Model with four values of the NH_3 mixing ratio.

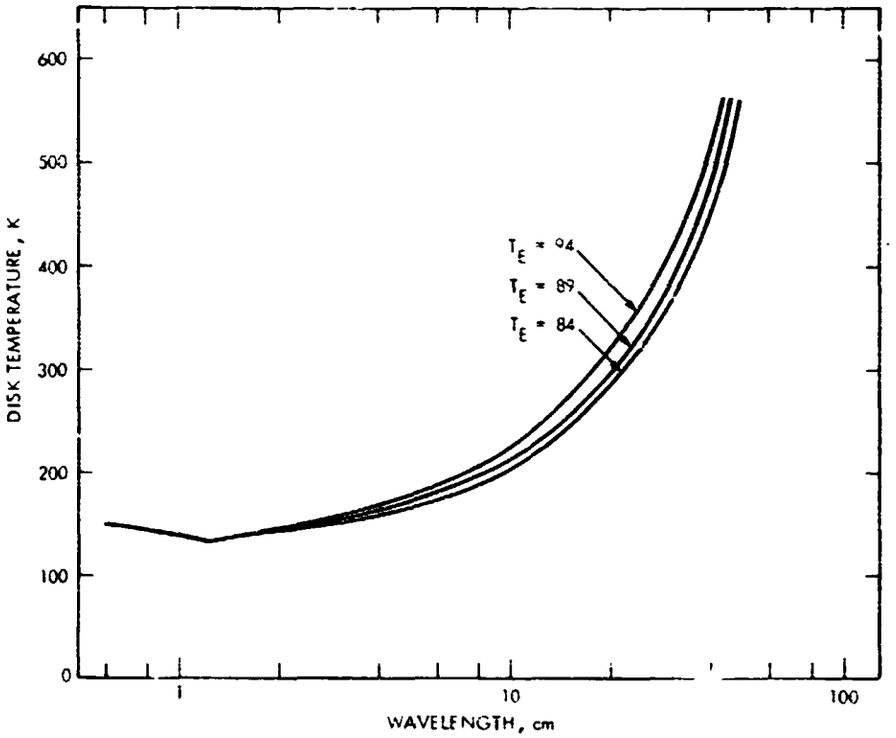

Figure 4. The effect of varying T_e, the effective temperature, on the computed microwave spectrum.

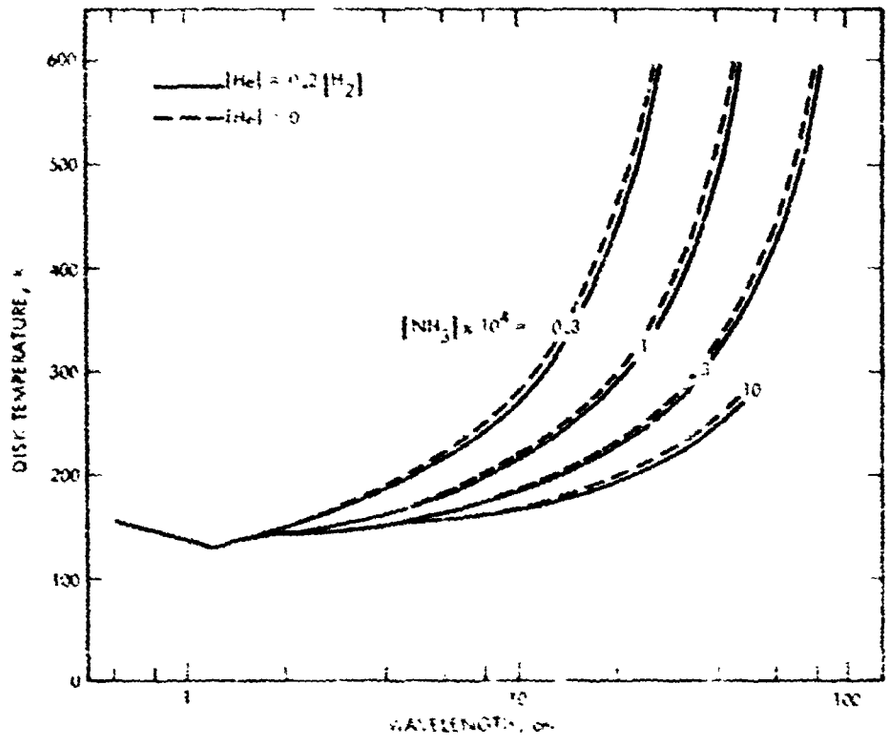

Figure 5. The effect of varying the helium abundance on the computed microwave spectra for four values of NH_3 mixing ratio (cf. Figure 3).

(from Weidenschilling and Lewis, 1973). In Figure 6 we show the calculated optical depth of this type of cloud as a function of frequency.

The result of the cloud model computation is shown in Figure 7. The solid curve is the spectrum of the model with no cloud ($\tau_o = 0$) and the dashed curve shows the effect of adding a cloud with $\tau_o \sim 1$. The trend is correct, i.e., the slope of the spectrum between ~6 and 21 cm is flattened just as the data tend to be; but the model curve misses the dense cluster of points near $\lambda = 21$ cm. Increasing the cloud opacity does not solve the discrepancy. The 21 cm temperature is only reduced an additional 2K when τ_o is doubled.

This very simple cloud approximation shows promise even though our first attempt failed to provide a good fit to the data. There is a need for further investigation of the vertical extent of the cloud model. Weidenschilling and Lewis (1973) suggest that cloud condensation might occur at altitudes above the saturation level, and that cloud particles might be swept up to higher altitudes by convection. These conditions would shift the peak of the cloud opacity to higher altitudes and lower temperatures. In a preliminary test, we computed the spectrum for $\tau_o = 1$ at the 250 K level and found that the 21 cm disk temperature was suppressed 10 K, bringing it into qualitative agreement with the observations.

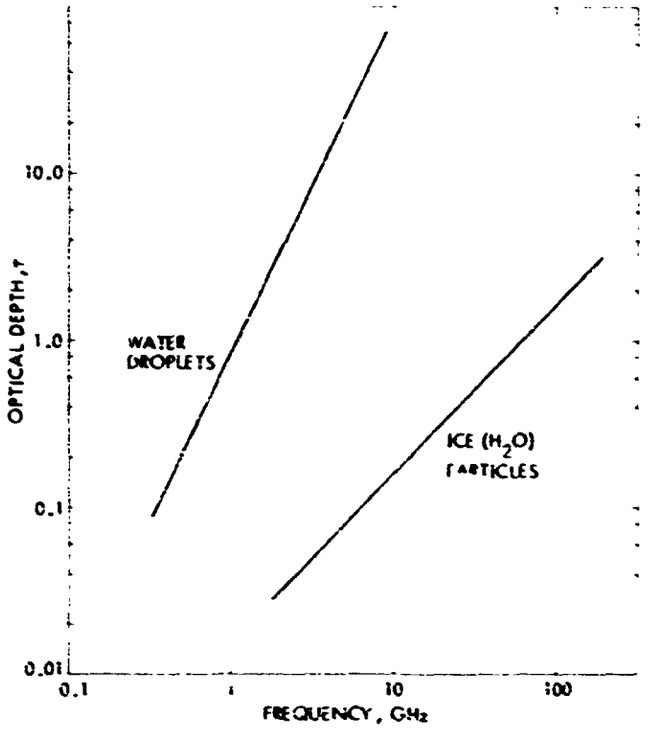

Figure 6. Opacity as a function of frequency computed for a cloud of water droplets with density 35 g/m³. Such a cloud has been postulated for Saturn by Weidenschilling and Lewis (1973).

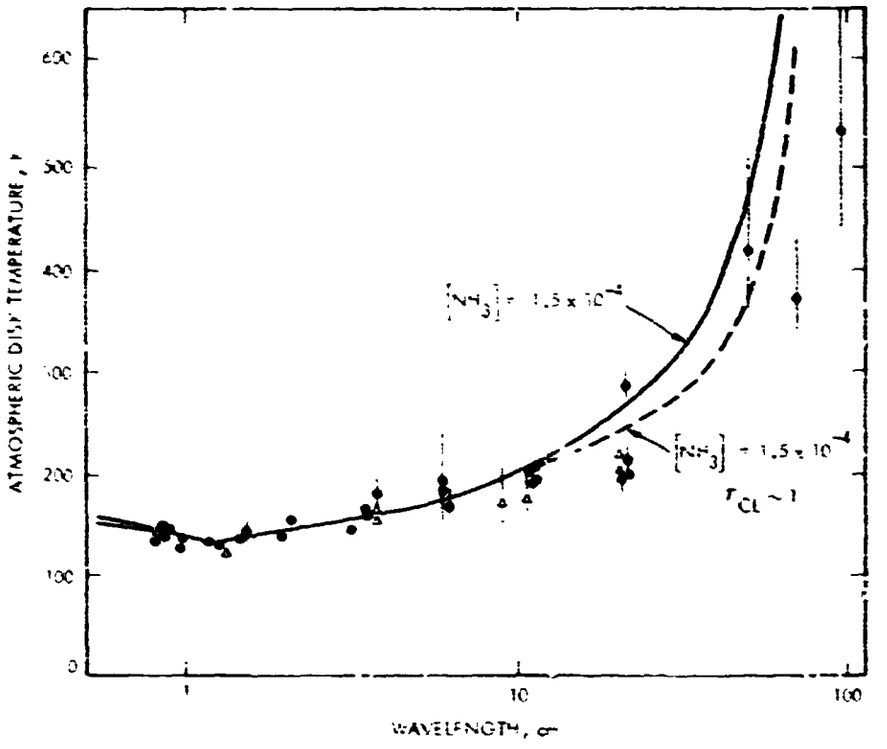

Figure 7. The microwave spectrum of Saturn's atmosphere compared with the nominal model. Curves for a solar value of NH_3 mixing ratio are shown with and without cloud opacity near the 270 K level of the atmosphere.

THE MILLIMETER SPECTRUM OF THE RINGS

The atmospheric models that fit the spectrum at centimeter wavelengths can be used to investigate the thermal spectrum of the rings at millimeter wavelengths. The atmospheric brightness temperatures, which are controlled by the ammonia opacity, are only weakly dependent on the exact choice of the NH_3 mixing ratio because the peak opacity at short radio wavelengths occurs near the cloud forming region where the ammonia is saturated. If we assume that the millimeter spectrum of the atmosphere is adequately determined by the models that fit the longer wavelength data, any excess emission at millimeter wavelengths can be attributed to thermal emission from the rings.

The short-wavelength data between 0.1 and 0.8 cm are shown with theoretical spectra in Figure 8. The solid curves represent the spectra for the two values of ammonia mixing ratio considered above, i.e., $[NH_3] = 1.5$ and 5×10^{-4}. The data have been corrected for ring obscuration and scattering effects, but the thermal component, T_t, is set to zero. The intent here is to demonstrate that these partially corrected temperatures are systematically higher than the model curves, which implies that the rings do emit thermally at millimeter wavelengths.

The dashed curves in Figure 8 demonstrate the magnitude of the increase in the computed microwave spectrum that occurs if the rings emit thermally. Because the thermal flux density received from the rings at a given frequency will vary with the solid angle of the ring surface, we show the computed spectra for two values of ring inclination. The ring brightness temperature spectrum shown in Figure 9 is assumed for these computations.

We obtain a ring brightness temperature spectrum by attributing the excess flux (measured minus predicted with $T_t = 0$) to thermal emission from the rings. The resulting spectrum is shown in Figure 9. Intrinsic thermal emission from the rings is indicated. The average of the excess temperatures between 1 mm and 2 mm, weighted by their absolute errors, gives $T_t \sim 25$ K. This result is consistent with the ring brightening from $T_t \sim 7$ K at 8.6 mm (Janssen and Olsen, 1978). An increase of thermal ring emission at millimeter wavelengths is not surprising since the brightness must approach ~95 K, the observed temperature at 10 μm. Furthermore, ice is a likely candidate for the ring particle composition, and its absorption coefficient increases markedly in the millimeter wavelength region.

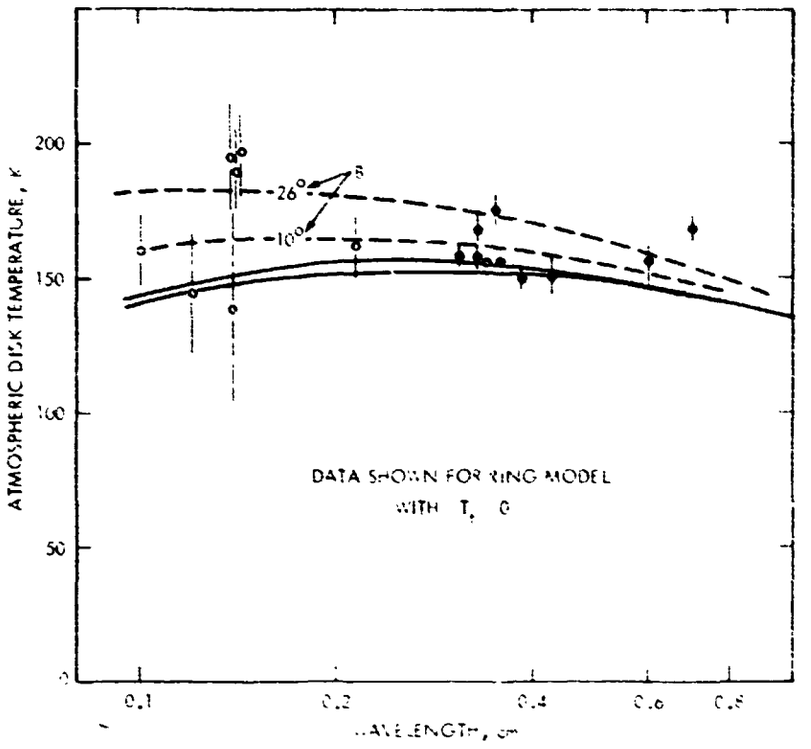

Figure 8. Saturn's 0.1-0.8 cm Spectrum with ring-model correction. The measured disk temperatures have been adjusted to account for the presence of the rings with the assumption that there is no thermal emission from the rings. The two solid curves represent the short wavelength spectra for the range of atmospheric models that fit the 0.8-100 cm microwave spectrum. The tendency for the data to fall systematically above the model spectra suggests that thermal emission from the rings is present. The two dashed curves show the increase in the computed spectra for two values of B and the ring spectrum shown in Figure 9.

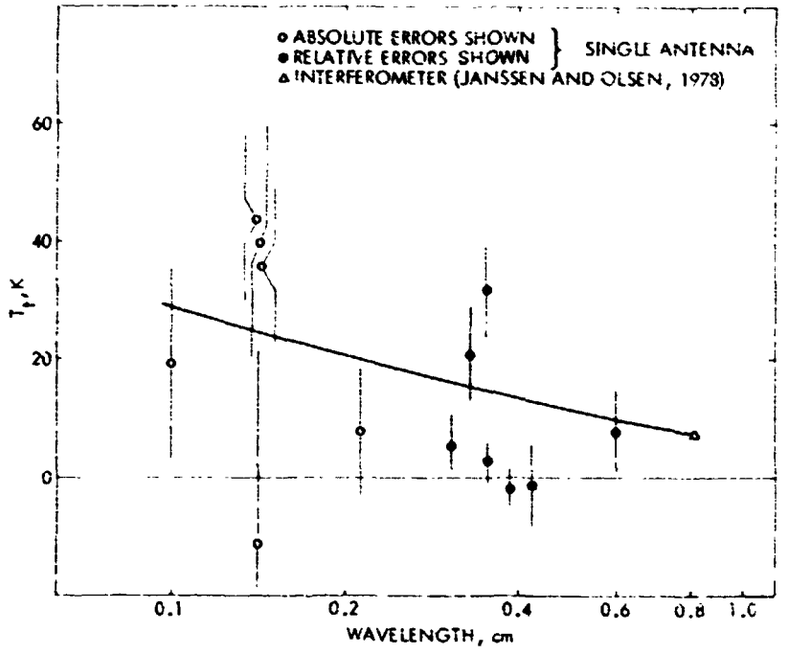

Figure 9. A millimeter spectrum for the thermal emission of Saturn's rings. The points are derived from the disk temperature measurements by assuming that the atmospheric spectrum is given by the $NH_3 = 5 \times 10^{-4}$ mixing ratio model, and that the excess observed emission may be ascribed to uniformly distributed thermal emission from the A and B rings. The curve is drawn to interpolate between the mean value $T_r = 25$ K at 0.14 cm and the interferometric determination at $T_r = 7$ K at 0.8 mm. Error bars from points shown as open circles are the given absolute errors, while the error bars from the points marked by filled circles show the given relative errors of measurement.

THE MICROWAVE SPECTRUM OF SATURN'S ATMOSPHERE

The microwave spectrum of the thermal emission from Saturn's atmosphere is shown in Figure 10. The effects of the rings have been removed from the data as discussed above. The nominal ring model was used with the ring brightness-temperature spectrum shown in Figure 9. Two model spectra are shown; the solid curve represents the computed spectrum with $[NH_3] = 5 \times 10^{-4}$, whereas the broken curve represents the spectrum for the model with a lower NH_3 abundance and the additional source of opacity near the 270 K level (i.e., an H_2O cloud).

There is good agreement between the model spectra and the ring-corrected data over the entire band, which spans three decades in wavelength. This agreement provides a strong argument that ammonia is present in Saturn's atmosphere, since NH_3 is the primary source of microwave opacity in the models. The shape of the spectrum in the wavelength interval centered on the 1.25 cm inversion band of NH_3 and the 130–135 K disk temperatures that are observed near the band center are in excellent agreement

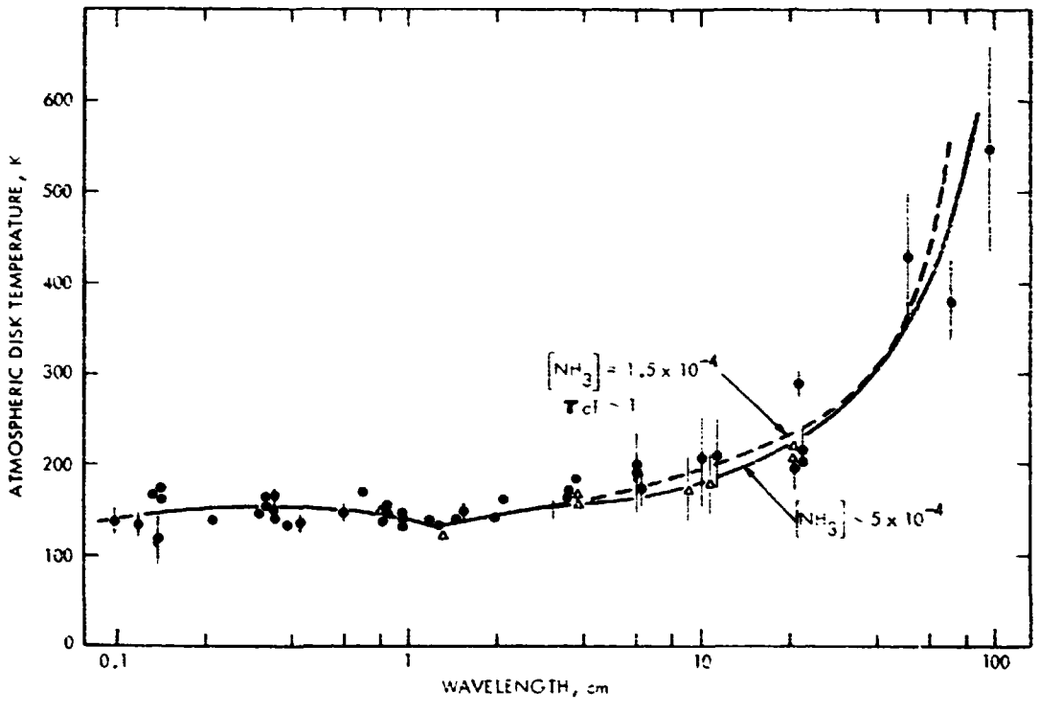

Figure 10. Saturn's microwave spectrum with data corrected for ring effects. Computed spectra are shown for the Nominal Model (Te = 89 K) for two values of ammonia mixing ratio, one with a cloud opacity near T = 270 K (dashed curve), and one without an additional source of opacity (solid curve).

with the models. Without the NH_3 opacity, these models yield disk temperatures in excess of 200 K at these wavelengths.

In the 10-21 cm region there is some evidence that the observed spectrum is slightly flatter than the model spectra. The agreement is good for both models shown, when one considers the statistical scatter in the data over the entire spectrum. Nevertheless, some improvement may be possible if more sophisticated cloud models are investigated and applied.

The model spectra at the longest wavelengths (>50 cm) are probably the most uncertain. Our assumptions regarding the absorption coefficient of the atmosphere at great depths, where temperatures and pressures exceed 1000 K and 1000 atmospheres, surely become invalid. Additional sources of opacity, e.g., from pressure induced ionization, may become important. A component of nonthermal emission from a Saturnian radiation belt is also plausible at these long wavelengths. Nevertheless, it is encouraging that the three measured temperatures are completely consistent with the relatively simple models that we have presented here.

ATMOSPHERIC TRANSMISSION LOSSES FROM A PROBE

With the models of Saturn's atmosphere in hand, one can readily compute the atmospheric attenuation that must be considered in the design of a probe communication system. We have performed the calculations for our nominal model atmosphere with a nominal ammonia mixing ratio of $[NH_3] = 3 \times 10^{-4}$. Cloud opacities were not included. The single-path absorption for three plausible probe frequencies are plotted as functions of pressure in Figure 11. The attenuation refers to the accumulated signal loss from a probe transmitting from a given pressure level in the atmosphere, e.g., a 2 GHz signal from the 10 atmosphere pressure level would be attenuated 4 db when transmitted vertically through the atmosphere.

A different representation of the results is shown in Figure 12, where we plot the vertical path absorption *vs* frequency for probe penetrations to pressure levels of 10, 30 and 100 atmospheres. We also show a computed attenuation curve (dashed line) for a probe in Jupiter's atmosphere. Note that the vertical attenuation to a given pressure level in the Jovian atmosphere is considerably less than the

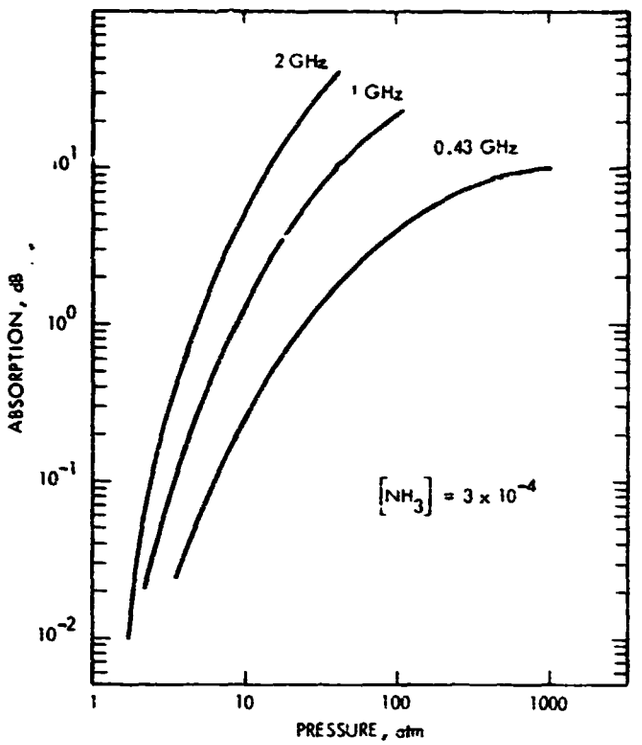

Figure 11. Vertical (single path) transmission loss in Saturn's atmosphere for plausible probe communication frequencies. The nominal atmospheric model with $(NH_3) = 3 \times 10^{-4}$ is assumed.

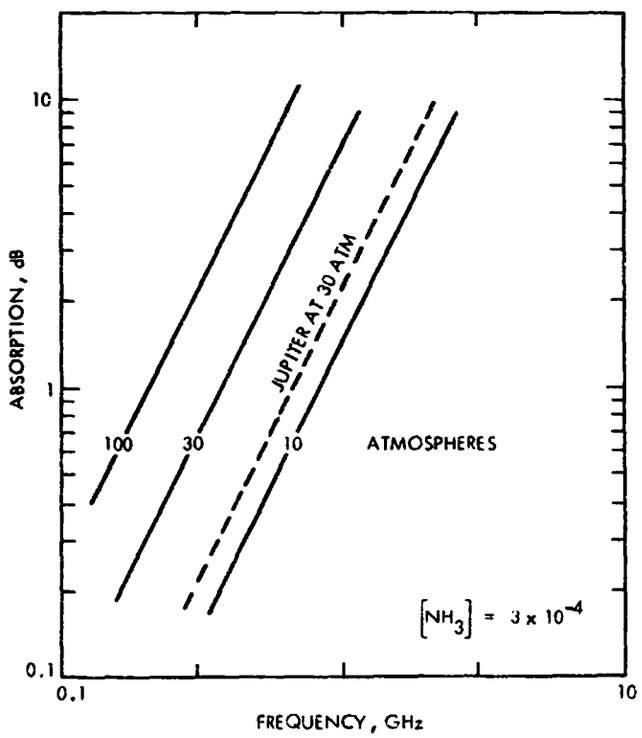

Figure 12. Vertical transmission loss from a probe at three pressure levels in Saturn's atmosphere. Computed loss vs. frequency is based on the nominal model atmosphere with ammonia mixing ratio = 3×10^{-4}. Dashed curve shows a similar attenuation vs. frequency curve for the 30 atmosphere level in Jupiter's atmosphere, where the predicted signal loss is not as great as in Saturn's atmosphere.

corresponding loss in Saturn's atmosphere. From the figure, we note that the "dB-loss" in Saturn's atmosphere is approximately three times greater. At 600 MHz, the vertical loss to 30 atmosphere pressure is 3 dB greater in Saturn's atmosphere. In general, the relation can be expressed as

$$\text{Loss dB}_{\text{Saturn}} \simeq 3 \times \text{Loss dB}_{\text{Jupiter}}. \qquad (2)$$

ACKNOWLEDGEMENTS

This paper is JPL atmospheres Publication Number 978-33 and represents one phase of research carried out at the Jet Propulsion Laboratory, California Institute of Technology, under Contract No. NAS 7-100, sponsored by the National Aeronautics and Space Administration.

REFERENCES

Baars, J. W. M., Genzel, R., Pauliny-Toth, I. I. K., and Witzel, A. (1977). *Astron. Astrophys. 61*, 99–106.
Berge, G. L. (1968). Recent observations of Saturn, Uranus, and Neptune at 3.12 cm. *Astrophys. Lett. 2*, 127–131.
Berge, G. L., and Read, R. B. (1968). The microwave emission of Saturn. *Astrophys. J. 152*, 755–764.
Berge, G. L., and Muhleman, D. O. (1973). High angular-resolution observations of Saturn at 12.1-centimeter wavelength. *Astrophys. J. 185*, 373–381.
Briggs, F. H. (1973). Observations of Uranus and Saturn by a new method of radio interferometry of fain moving sources. *Astrophys. J. 182*, 999–1011.
Caldwell, J. (1977). The atmosphere of Saturn: An infrared perspective. *Icarus 30*, 493–510.
Condon, J. J., Yerbury, M. J., and Jauncey, D. L. (1974). Interpretation of Saturn's decimetric radio emission. *Astrophys. J. 193*, 257–261.
Courtin, R., Coron, N., Encrenaz, Th., and Gispert, R. (1977). Observations of giant planets at 1.4 mm and consequences on the effective temperatures. *Astron. Astrophys. 60*, 115–123.
Cuzzi, J. N., and Dent, W. A. (1975). Saturn's rings: The determination of their brightness temperature and opacity at centimeter wavelengths. *Astrophys. J. 198*, 223–227.
Davies, R. D., Beard, M., and Cooper, B. F. C. (1964). Observations of Saturn at 11.3 centimeters. *Phys. Rev. Letters 13*, 325–327.
Dent, W. A. (1972). A flux-density scale for microwave frequencies. *Astrophys. J. 177*, 93–99.
Drake, F. D. (1962). Microwave spectrum of Saturn. *Nature 195*, 893–894.
Epstein, E. E., Dworetsky, M. M., Montgomery, J. W., Fogarty, W. G., and Schorn, R. A. (1970). Mars, Jupiter, Saturn and Uranus: 3.3 mm brightness temperatures and a search for variations with time and phase angle. *Icarus 13*, 276–281.
Epstein, E. E. (1978). Private Communication.
Gary, B. L. (1974). Jupiter, Saturn, and Uranus disk temperature measurements at 2.07 and 3.56 cm. *Astron. J. 79*, 318–320.
Gerard, E., and Kazes, I. (1973). Observations of Saturn at wavelengths of 6.2, 11.1 and 21.2 cm. *Astrophys. Lett. 13*, 181–184.
Gulkis, S., McDonough, T. R., and Craft, H. (1969). The microwave spectrum of Saturn. *Icarus 10*, 421–427.
Gulkis, S., and Poynter, R. L. (1972). Thermal radio emission from Jupiter and Saturn *Phys. of Earth and Planetary Interiors* 6, 36–43.
Hobbs, R. W., and Knapp, S. L. (1971). Planetary temperatures at 9.55 mm wavelength. *Icarus 14*, 204–209.
Hughes, M. P. (1966). Planetary observations at a wavelength of 6 cm. *Planet. Space Sci. 14*, 1017–1022.
Janssen, M. A., and Olsen, E. T. (1978). A measurement of the brightness temperature of Saturn's rings at 8 mm wavelength. *Icarus 33*, 263–278.
Kellermann, K. I. (1966). The thermal radio emission from Mercury, Venus, Mars, Saturn and Uranus. *Icarus 5*, 478–490.
Klein, M. J., and Gulkis, S. (1978). Jupiter's atmosphere· Observations and Interpretation of the microwave spectrum near 1.25 cm wavelength. *Icarus*. In press.
Kostenko, V. I., Pavlov, A. V., Sholomitsky, G. B., Slysh, V. I., Soglasnova, V. A., and Zabolotny, V. F. (1971). The brightness temperature of planets at 1.4 mm. *Astrophys. Lett. 8*, 41–42.
Kuzmin, A. D., and Losovskii, B. Ya. (1971). Measurements of 8.2 mm radio emission from Saturn and estimate of the rings optical thickness. *Astron. Vestnik 5*, 78–81.

REFERENCES (Contd)

Low, F. J., and Davidson, A. W. (1965). Lunar observations at a wavelength of 1 millimeter. *Astrophys J. 142*, 1278–1282

Ohring, G., and Lacser, A. (1976). The ammonia profile in the atmosphere of Saturn from inversion of its microwave emission spectrum. *Astrophys. J. 206*, 622–626.

Pauliny-Toth, I. I., and Kellermann, K. I. (1970) Millimeter-wavelength measurements of Uranus and Neptune. *Astrophys. Lett. 6*, 185–187.

Rather, J. D. G., Ulich, B. L., and Ade, P. A. R. (1974) Planetary brightness temperature measurements at 1.4 mm wavelength. *Icarus 22*, 448–453.

Schloerb, F. P. (1977). Radio Interferometric investigations of Saturn's rings at 3.71 and 1.30 cm wavelengths. Ph.D. Thesis, California Institute of Technology.

Seling, T. V. (1970). Observations of Saturn at 3.75 cm *Astron. J. 75*, 67–68

Turegano, J. A. and Klein, M. J. (1978). Paper in preparation.

Ulich, B. L., Cogdell, J. R., and Davis, J. H. (1973). Planetary brightness temperature measurements at 8.6 mm and 3.1 mm wavelengths. *Icarus 19*, 59–82.

Ulich, B. L. (1974). Absolute brightness temperature measurements at 2 1 mm wavelength. *Icarus 21*, 254–261.

Ulich, B. L. (1978). Private Communication.

Voronov, V. N., Kislyakov, A. G., and Troitskii, A. V. (1974). Brightness Temperatures of Venus, Saturn, and Mercury at 3.87 mm. *Astron. Vestnik 8*, 17–19.

Ward, D. B. (1977). Far infrared spectral observations of Saturn and its rings. *Icarus 32*, 437–442.

Weidenschilling, S. J., and Lewis, J. S. (1973) Atmospheric and cloud structures of the Jovian planets. *Icarus 20*, 465–476.

Welch, W. J , Thornton, D. D., and Lohman, R. (1966). Observations of Jupiter, Saturn, and Mercury at 1.53 centimeters. *Astrophys. J. 146*, 799–809.

Werner, M. W., Neugebauer, G., Houck, J. R., and Hauser, M. G. (1978). One millimeter brightness temperatures of the planets NASA-TM-[illegible]. 21 pp.

Wrixon, G. T., and Welch, W. J. (1970). The millimeter wave spectrum of Saturn. *Icarus 13*, 163–172.

Yerbury, M. J., Condon, J. J , and Jauncey, D. L. (1971). Observations of Saturn at a wavelength of 49.5 cm. *Icarus 15*, 459–465.

Yerbury, M. J., Condon, J. J., and Jauncey, D. L. (1973). The brightness temperature of Saturn at decimeter wavelengths. *Icarus 18*, 177–180.

DISCUSSION

J. WARWICK: Mike, do you see any evidence for possible synchrotron emission in this spectrum?

M. KLEIN: There's no compelling evidence. What we see is that even at wavelengths near 90 cm there doesn't seem to be any excess in the brightness temperature. But there could be some contribution due to synchrotron emission because as we get down to 90 cm the thermal models are rather uncertain. The ammonia absorption coefficient is not well known at several thousand degrees temperature and thousands of atmospheres of pressure. However, all I can say is that we see no compelling reason to assume that we need synchrotron radiation to explain the spectrum.

D. CRUIKSHANK: In the models and the observations of the Jupiter microwave spectrum, the ammonia line at 1.25 cm is fairly pronounced. Is there some simple-minded reason why that doesn't show up very strongly either in the observations or the models of Saturn?

M. KLEIN: For Saturn we have a higher-pressure model than we had for Jupiter because the lapse rate is different. Then since we are looking at a higher pressure, the line is spread out by collisional broadening.